CrossMark click for updates

View Article Online
View Journal

INORGANIC CHEMISTRY FRONTIERS

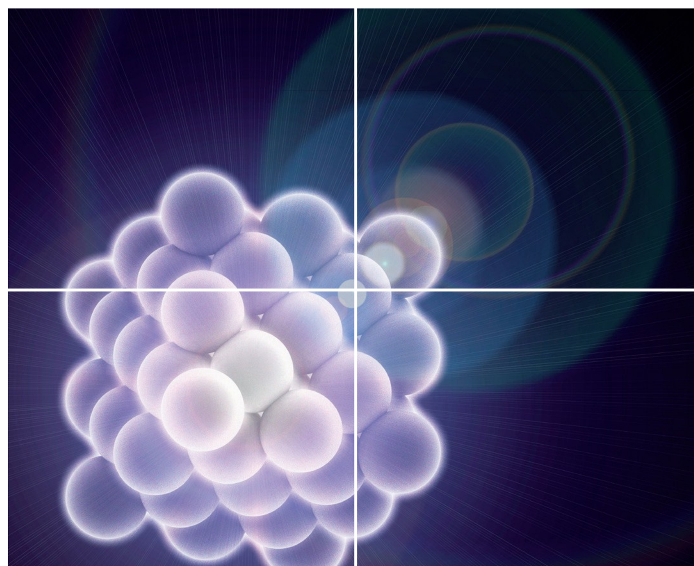

Accepted Manuscript

This article can be cited before page numbers have been issued, to do this please use: S. Perumal, S. Roychowdhury and K. Biswas, *Inorg. Chem. Front.*, 2015, DOI: 10.1039/C5QI00230C.

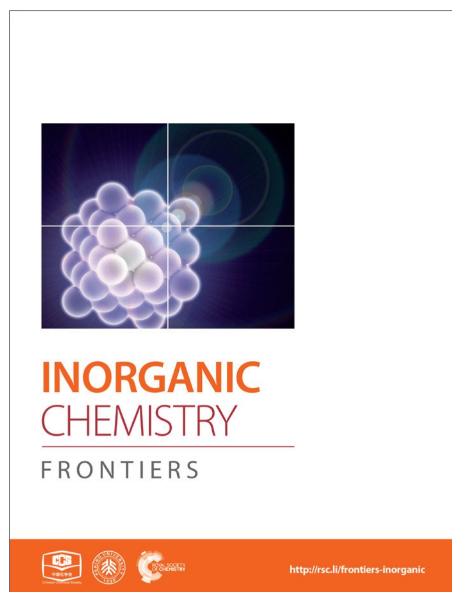

This is an *Accepted Manuscript*, which has been through the Royal Society of Chemistry peer review process and has been accepted for publication.

Accepted Manuscripts are published online shortly after acceptance, before technical editing, formatting and proof reading. Using this free service, authors can make their results available to the community, in citable form, before we publish the edited article. We will replace this *Accepted Manuscript* with the edited and formatted *Advance Article* as soon as it is available.

You can find more information about *Accepted Manuscripts* in the **Information for Authors**.

Please note that technical editing may introduce minor changes to the text and/or graphics, which may alter content. The journal's standard **Terms & Conditions** and the **Ethical guidelines** still apply. In no event shall the Royal Society of Chemistry be held responsible for any errors or omissions in this *Accepted Manuscript* or any consequences arising from the use of any information it contains.

中国化学会 Chinese Chemical Society
PEKING UNIVERSITY 1898
ROYAL SOCIETY OF CHEMISTRY
http://rsc.li/frontiers-inorganic

View Article Online
DOI: 10.1039/C5QI00230C

Reduction of thermal conductivity through nanostructuring enhances the thermoelectric figure of merit in $Ge_{1-x}Bi_xTe$

Suresh Perumal,† Subhajit Roychowdhury,† and Kanishka Biswas *

New Chemistry Unit, Jawaharlal Nehru Centre for Advanced Scientific Research (JNCASR), Jakkur P.O., Bangalore 560064 (India)

†*SP and SR hold equal first authorship*

**E-mail: kanishka@jncasr.ac.in*

Published on 18 November 2015. Downloaded on 29/11/2015 10:35:46.

Abstract. Promising thermoelectric figure of merit, zT, of ~ 1.3 at 725 K was achieved in high quality crystalline ingot of $Ge_{1-x}Bi_xTe$ samples. Substitution of Bi^{3+} in Ge^{2+} sublattice of GeTe significantly reduces the excess hole concentration due to aliovalent donor dopant nature of Bi^{3+}. Reduction in carrier density optimizes the electrical conductivity, and subsequently enhances the Seebeck coefficient in $Ge_{1-x}Bi_xTe$. More importantly, low lattice thermal conductivity of ~1.1 W/mK for $Ge_{0.90}Bi_{0.10}Te$ was achieved, which is due to the collective phonon scattering from meso-structured grain boundaries, nano-structured precipitates, nano-scale defect layers, and solid solution point defects. We have obtained reasonably high mechanical stability of $Ge_{1-x}Bi_xTe$ samples. Measured Vickers microhardness value of the high performance sample is ~165 H_v, which is comparatively higher than that of state-of-art thermoelectric materials, such as PbTe, Bi_2Te_3, and Cu_2Se.

Inorganic Chemistry Frontiers Accepted Manuscript

View Article Online
DOI: 10.1039/C5QI00230C

Published on 18 November 2015. Downloaded on 29/11/2015 10:35:46.

Inorganic Chemistry Frontiers Accepted Manuscript

INTRODUCTION

Thermoelectric (TE) materials have the potential to play a predominant role in future energy management by converting the fractions of waste heat into the useful electricity.[1-4] The conversion efficiency of TE materials are determined by the material's thermoelectric figure of merit, $zT = S^2\sigma T/\kappa_{total}$, where, S, σ, κ_{total} and T are the Seebeck coefficient, electrical conductivity, total thermal conductivity and temperature, respectively. Decoupling of these interdependent parameters, S, σ, and κ_{total}, are of great challenge to enhance the zT. Nevertheless, significant attempts are made to increase the zT by enhancing the power factor, $S^2\sigma$, *via* minority carriers energy filtering,[5a] the formation of resonance energy levels and degenerate states close to the Fermi level (E_F),[5b,5c] valence and conduction band convergence,[5d-5g] and quantum confinement effect.[5f] In addition, substantial efforts are taken on to reduce the lattice thermal conductivity by increasing the phonon scattering *via* introducing solid solution point defects, embedding of endotaxial nano-inclusions as second phases in the matrix,[6,7a] forming the meso-scale grain boundaries[7] and due to intrinsic bond anharmonicity.[8]

IV-VI metal chalcogenides, PbTe, SnTe and GeTe, are regarded as the present state-of-art high performance thermoelectric materials that are capable to work in the intermediate temperature range of 600-900 K.[1, 3, 5, 6, 7] Amongst, well-known PbTe based materials have been extensively studied from the materials aspect to the device level; however, toxic nature of Pb limits its usage in terms of the large scale thermoelectric applications.

GeTe is being regarded as one of the known promising p-type narrow band gap thermoelectric materials since 1960s;[9] but it has not attracted much attention due to its large p-type carrier density (~10^{21} cm^{-3}) that comes from its intrinsic Ge vacancy.[10] High carrier concentration in GeTe resulted in high electrical conductivity of ~8500 S/cm, low Seebeck coefficient value of ~30 μV/K, and perversely high total thermal conductivity of ~8 W/mK at

View Article Online
DOI: 10.1039/C5QI00230C

300 K, thus leading to a maximum *zT* value of 0.7 at 720 K.[11] Undoped GeTe undergoes the ferroelectric structural phase transition from high temperature cubic (*β*-phase) to low temperature rhombohedral (*α*- phase) at ~700 K due to the thermal strain induced shift in Ge atoms (**Fig. 1a**), which thrusts the distortion in the unit cell along [111] direction with an angular distortion of α = 1.65°.[12]

GeTe-rich composition with $AgSbTe_2$, recognized as TAGS-80 $[(GeTe)_{0.80}(AgSbTe_2)_{0.20}]$ and TAGS-85 $[(GeTe)_{0.85}(AgSbTe_2)_{0.15}]$, are being considered as the traditional thermoelectric material with reasonably high zT of 1.3.[13] Recently, $Ge_xPb_{1-x}Te$ is reported to be high performance thermoelectric materials due to the donor dopant nature of Pb which significantly increases Seebeck coefficient by reducing the carrier density, and furnish low thermal conductivity generated from the thermodynamically driven various nanoscale modulations.[14] *zT* of ~1.9 at 773 K was obtained in 3mol% Bi_2Te_3 doped $Ge_{0.87}Pb_{0.13}Te$ samples due to the thermal conductivity reduction from point defect scattering of phonons and enhancement of power factor through valence band convergence.[15] 3 mol% Bi_2Te_3 doping in $Ge_{0.87}Pb_{0.13}Te$ promoted the solubility of PbTe in GeTe and enhances the valence band convergence. Composition variation and thermal treatment in Ge-Sb-Te based alloys were resulted the parquet-like nanoscale defect layers and meso-structured domain variants, twin and inversion boundaries, which significantly reduces the lattice thermal conductivity, thus led to the maximal *z*T values of ~1.9.[16] Moreover, a recent report on Sb doping in GeTe resulted in significantly high *z*T of ~1.85 and high mechanical stability compared to that of other thermoelectric materials.[16a] Motivated by the low thermal conductivity, high *z*T and enhanced mechanical stability of Sb doped GeTe, here an attempt has been made to understand the effect of Bi doping on thermoelectric performance and mechanical stability of GeTe.

Published on 18 November 2015. Downloaded on 29/11/2015 10:35:46.

Inorganic Chemistry Frontiers Accepted Manuscript

View Article Online
DOI: 10.1039/C5QI00230C

Here, we report the promising thermoelectric performance and reasonably high mechanical stability of $Ge_{1-x}Bi_xTe$ (x = 0-0.10) samples. Substitution of Bi in GeTe decreases the holes concentration due to its donor dopant nature, which optimizes Seebeck coefficient and electronic transport properties. We have achieved low lattice thermal conductivity of ~1.1 W/mK for $Ge_{0.90}Bi_{0.10}Te$, which is reasonably lower compared with other high performance GeTe based materials. Significant thermal conductivity reduction was achieved due to collective phonon scattering from meso-structured grain boundaries, nano-structured precipitates, nano-structured defect layers, and solid solution point defects. The maximum figure of merit, zT, of ~1.3 was achieved for the composition of $Ge_{0.94}Bi_{0.06}Te$ at 725 K. Additionally, Vickers microhardness value of ~165 H_V was measured for $Ge_{0.94}Bi_{0.06}Te$ sample, which is significantly higher than pristine GeTe (~145 H_V) and other state-of-art thermoelectric materials, such as PbTe, SnTe and Bi_2Te_3 based materials.

EXPERIMENTAL SECTION

Reagents. Germanium (99.995%), bismuth (99.9999%) and tellurium (99.999%) were used for synthesis without further purification.

Synthesis. High quality crystalline ingots (~ 6 g) of $Ge_{1-x}Bi_xTe$ (x=0−0.10) were prepared by vacuum sealed quartz tube (10^{-6} Torr) melting reaction of stoichiometric amount of starting elements of Ge, Bi and Te. Typically, to synthesize the $Ge_{0.94}Bi_{0.06}Te$ sample, Ge (1.9692 g, 27.109 mmol), Bi (0.3625 g, 1.735 mmol), and Te (3.6749 g, 28.800 mmol) were added in a quartz tube of 10 mm diameter. The tube was sealed under vacuum (10^{-6} Torr) and slowly heated to 1223 K over 10 h then soaked for 6 h, and slowly cooled down to room temperature over 10 h. Density of the all samples was measured by Archimedes' methods, which was ~99% of theoretical density (~6.18 g/cc). In order to measure the thermoelectric properties, ingots were sliced into pellets and bars by using low speed diamond saw (**Fig. 1a**).

Published on 18 November 2015. Downloaded on 29/11/2015 10:35:46.

Inorganic Chemistry Frontiers Accepted Manuscript

View Article Online
DOI: 10.1039/C5QI00230C

Powder X-ray diffraction. Powder X-ray diffraction patterns were recorded for the finely ground samples using a Cu-Kα (λ = 1.5406 Å) radiation on a Bruker D8 diffractometer.

Band gap measurement. To estimate optical band gap of the as-synthesized samples, diffuse reflectance measurement has been done with finely ground powder at room temperature using FT-IR Bruker IFS 66V/S spectrometer in the wave number range 4000-400 cm^{-1} with 2 cm^{-1} resolution and 50 scans. Absorption (α/Λ) data were calculated from reflectance data using Kubelka-Munk equation: $\alpha/\Lambda=(1-R)^2/(2R)$, where R is the reflectance, α and Λ are the absorption and scattering coefficient, respectively. The energy band gaps were derived from α/Λ vs. E_g (eV) plot.

Transmission electron microscopy. Aberration corrected FEI TITAN 3™ 80-300 KV transmission electron microscope was used to investigate the nanostructure in $Ge_{1-x}Bi_xTe$ sample. Samples were prepared by mechanical polishing and followed by the ion beam polishing/milling to achieve thin foil of ~20-80 nm. Bright field imaging, high resolution TEM imaging and selected area electron diffraction (SAED) were carried out using TEM.

Electrical Transport. Electrical conductivity and Seebeck coefficients were measured simultaneously under He atmosphere from room temperature to 773 K on a ULVAC-RIKO ZEM-3 instrument system. The typical sample for measurement had a parallelepiped shape with the dimensions of ~2×2×8 mm^3. The longer direction coincides with the direction in which the thermal conductivity was measured. Heating and cooling cycles of transport data confirmed the thermal stability (**Fig. S1**, Supporting Information).

Hall measurement. Hall measurement was carried out at room temperature in the home made setup, where fixed magnetic field and dc-current were used to be 0.25 T and 5 mA, respectively. The carrier concentration (n) was calculated from the equations of $n = 1/(eR_H)$, where R_H is the Hall coefficient and e is the electron charge.

Published on 18 November 2015. Downloaded on 29/11/2015 10:35:46.

Inorganic Chemistry Frontiers Accepted Manuscript

View Article Online
DOI: 10.1039/C5QI00230C

Thermal conductivity. Thermal diffusivity, D, was directly measured in the range 300–773 K by using the laser flash diffusivity method in a Netzsch LFA-457 (**Fig. S2**, Supporting Information). Coins with ~8 mm diameter and ~2mm thickness were used in all of the measurements. Temperature dependent heat capacity, C_p, was derived using standard sample (pyroceram) in LFA-457, which is in good agreement with Dulong-Petit C_p value (**Fig. S3**, Supporting Information). The total thermal conductivity, κ_{total}, was calculated using the formula $\kappa_{\text{total}} = DC_p\rho$, where ρ is the density. The measured densities of all the samples were about 99% of theoretical density (6.18 g/cc)

Mechanical properties. Microhardness of all the samples was measured on the Vickers hardness scale using the diamond indenter by means of commercial Zwick Roell ZHU 2.5 instrument. The applied force and holding time were kept to be 2 N and 10s, respectively. Vickers hardness values (kgf/mm^2) were determined from the equation of H_v = 1. 854xL/(2d)^2, where L is the indentation load and 2d is the diagonal length of the indentation. Vickers microhardness impressions of the indenter after unloading are shown in **Fig. S4** (see Supporting Information). The uncertainty of microhardness measurement is about 5%.

Published on 18 November 2015. Downloaded on 29/11/2015 10:35:46.

RESULT AND DISCUSSIONS

Crystalline ingots of $Ge_{1-x}Bi_xTe$ (x = 0.00, 0.02, 0.06 and 0.10) were synthesized by vacuum sealed tube melting reaction and the structural properties were analysed using powder X-ray diffraction (PXRD). **Fig. 1b** presents PXRD patterns of $Ge_{1-x}Bi_xTe$, which could be indexed based on rhombohedral GeTe ($R3m$) structure. Typically, presence of double peaks in the range 2θ = 23° to 27° and 2θ = 41° to 45° further confirms the rhombohedral phase. Additionally, substitution of Bi in GeTe tends to merge these double peaks into single peak (See **Fig. 1c**). Substitution of Bi tries to rearrange the positions of Ge from (½-x ½-x ½-x) to (½ ½ ½), which indicates that the cubic nature of the system increases

Inorganic Chemistry Frontiers Accepted Manuscript

View Article Online
DOI: 10.1039/C5QI00230C

with Bi doping in GeTe. Similar result was observed previously in the case of Sb doped GeTe.[16a]

Spectroscopically measured band gaps of $Ge_{1-x}Bi_xTe$ samples are shown in **Fig. 1d**. Optical band gap of pure GeTe is observed to be ~ 0.21 eV. Substitution of Bi at GeTe substantially reduces the band gap from ~0.21 eV to 0.08 eV (**Fig. 1d**). In GeTe, Te (electronegativity~2.10 in Pauling scale) forms valence band, whereas Ge (electronegativity ~2.01) contributes to the conduction band. The reduction in band gap is due to the formation of Bi states below the conduction band because of its donor dopant nature and the slightly higher electronegativity of Bi (~ 2.02) compared to Ge. Previously reported first principle electronic structure calculations also indicated the decreases in the band gap of GeTe after Bi doping due to lowering of conduction band energy.[17]

Nano/microstructures of $Ge_{0.90}Bi_{0.10}Te$ are investigated by aberration corrected TEM and are shown in **Fig. 2**. Low magnification TEM micrograph of $Ge_{0.9}Bi_{0.1}Te$ is presented in **Fig. 2a,** which clearly shows the presence of nanoprecipitates with dark contrast in the matrix of GeTe. In **Fig. 2b**, high magnification micrograph illustrates ~100-200 nm sized fine grains of GeTe (marked in yellow dotted circle). Nanoprecipitates with size in the range 5-20 nm are observed in high resolution TEM micrograph in **Fig.2c**. Although it was really difficult to determine actual composition of the nanoprecipiates by energy dispersive X-ray spectroscopy, but we speculate that the nanoprecipitates are indeed Bi rich phases which are embedded in GeTe matrix. Presence of the nanoscale parallel cation-position like defect layers in the van der Waals gaps are also clearly seen throughout the samples (see **Fig.2d**). These defect layers are formed because of strongly disordered octahedral voids between the successive Te-Te layers. Moreover, inset of **Fig. 2d** shows the diffused selected area diffraction pattern (SAED), which is obtained from the defect layers region. Additionally, these defects seemed to be thermodynamically less stable as it disappears upon prolonging

Published on 18 November 2015. Downloaded on 29/11/2015 10:35:46.

Inorganic Chemistry Frontiers Accepted Manuscript

View Article Online
DOI: 10.1039/C5QI00230C

exposure of high energy electron beam, even for 1 min exposure. **Fig.2e** illustrates the HRTEM micrographs of defect-free region, zoomed area from **Fig.2d**, with corresponding SAED pattern with clear spots (inset of **Fig.2e**). HRTEM micrograph on defect-free region illustrates the interplanar spacing of ~0.34 nm that corresponds to (021) lattice planes of GeTe, (see **Fig.2f**), which further confirms rhombohedra *R3m* phase. Defect-free regions shows the clearly separated diffraction spots (see inset **Fig. 2f**).

Fig. 3a presents the electrical conductivity, σ, of $Ge_{1-x}Bi_xTe$ (x = 0-0.10) samples as a function of temperature. The σ of all the samples decreases with increasing the temperature, which is typically observed for the degenerate semiconductors. Pristine GeTe exhibits the σ value of ~8067 S/cm at 300 K, which decreases to ~2158 S/cm at 708 K. Around 673 K, σ vs. T data shows an anomaly which is due to structural transition (*R3m* to *Fm-3m*) in GeTe. Furthermore, addition of Bi of 10 mol% in GeTe drastically reduces the σ value from ~8067 S/cm to ~986 S/cm, due to the reduction in the carrire concentration. Hall measurement was performed to measure the room temperature hole concentration. Typically, the calculated carrier density, *n*, is ~8.7 x 10^{20} cm^{-3} GeTe which decreases to ~1.24 x10^{20} cm^{-3} for $Ge_{0.94}Bi_{0.06}Te$, respectively. This reduction in *p*-type carrier concentration is attributed to the aliovalent dopant nature of Bi^{3+}at Ge^{2+} site in GeTe which gives rise to the extra electron to the system.

Fig. 3b presents the Seebeck coefficient value, *S*, of $Ge_{1-x}Bi_xTe$ (x = 0- 0.10) samples as a function of temperature. For all the samples, positive sign of the *S* indicate that holes are responsible for thermoelectric transport, which supports the Hall coefficient data. At 300 K, GeTe has the *S* value of ~34 μV/K which increases with temperature, then reaches to ~153 μV/K at 708 K.[11a] It is expected that doping of Bi in GeTe would increase the *S* value as it drastically reduces the holes concentration. Typically, 10 mol % of Bi doping in GeTe increases the *S* value to ~98 μV/K at 300K, which reaches to maximum value ~236 μV/K at

Published on 18 November 2015. Downloaded on 29/11/2015 10:35:46.

Inorganic Chemistry Frontiers Accepted Manuscript

View Article Online
DOI: 10.1039/C5QI00230C

708 K. Increase of Seebeck coefficient by Bi substitution is mainly due to decreases in hole concentration, which will be clear from Pisarenko plot (next section).

Fig.3c shows the measured Seebeck values, S, as a function of holes density, n, for GeTe and $Ge_{0.94}Bi_{0.06}Te$, which are compared with the Pisarenko plot at different temperatures of 323 K and 623 K.[14a, 14d, 15, 16] We have also compared the present S vs. n data with previously reported other high performance GeTe based materials such as, $Ge_{1-x}Sb_xTe$,[16a] $(GeTe)_{1-x}[(PbTe)(SnTe)(Bi_2Te_3)]_x$,[14a] $Ge_{1-x}Pb_xTe$,[14d] and 3mol% Bi_2Te_3 doped $Ge_{0.87}Pb_{0.13}Te$.[15] S vs. n data of $Ge_{1-x}Bi_xTe$ follows the Pisarenko relation, which indicates enhancement in Seebeck coefficient upon Bi doping in GeTe is mainly due to decreases in carrier concentration.

Fig.3d illustrates the power factor, $S^2\sigma$, of $Ge_{1-x}Bi_xTe$ (x = 0-0.10) samples as a function of temperature. Typically, $Ge_{0.94}Bi_{0.06}Te$ samples shows $S^2\sigma$ value of ~12 $\mu Wcm^{-1}K^{-2}$ at 300K, which reaches to maximum ~40 $\mu Wcm^{-1}K^{-2}$ at 712 K. Though S values increases upon Bi doping in GeTe, it does not improve the $S^2\sigma$ values due to large reduction in electrical conductivity.

Fig. 4a presents the total thermal conductivity, κ_{total}, of $Ge_{1-x}Bi_xTe$ (x = 0-0.10) samples as a function of temperature. Typically, pristine GeTe has the κ_{total} value of ~8.3 W/mK at 300 K, which decreases to ~3.4 W/mK at 673 K. Mention must be made that increase in κ_{total} above 673 K in undoped GeTe is due to the rhombohedral to cubic structural phase transition. This trend was earlier observed for other GeTe based materials.[16a] With increasing the Bi concentration, the κ_{total} drastically reduces from ~8.3 W/mK for GeTe to ~1.6 W/mK for $Ge_{0.90}Bi_{0.10}Te$ at 300 K.

The electronic thermal conductivity, κ_e, as a function of temperature for $Ge_{1-x}Bi_xTe$ (x = 0-0.10) were presented in **Fig. S5** (see supporting information). κ_e was calculated *via* Wiedemann-Franz law, $\kappa_e = \sigma \cdot L \cdot T$, where L is the Lorenz number. L, can be obtained based

Published on 18 November 2015. Downloaded on 29/11/2015 10:35:46.

Inorganic Chemistry Frontiers Accepted Manuscript

View Article Online
DOI: 10.1039/C5QI00230C

on the fitting of the respective Seebeck values that estimate the reduced chemical potential assuming single parabolic band model as per equation (1) (**Fig. S6**, SI).[8c,18]

$$L = \left(\frac{k_b}{e}\right)^2 \frac{3F_0(\eta)F_2(\eta) - 4F_1(\eta)^2}{F_0(\eta)^2} \qquad (1)$$

Pristine GeTe has the κ_e value of ~5.6 W/m.K at 300 K, which suggests that carriers are mainly responsible for heat transport in GeTe. Due to the donor dopant nature of Bi in GeTe, it reduces the *p*-type carrier density and significantly decreases the κ_e. Typically, 10 mole % of Bi in GeTe reduces the κ_e value from 5.66 W/mK to 0.58 W/mK, which is about 90% reduction as compared to undoped GeTe.

The κ_{lat} of all the samples was obtained by subtracting the κ_e from κ_{total} (**Fig. 4b**). κ_{lat} value of $Ge_{1-x}Bi_xTe$ decrease with increase the Bi concentration. At 300 K, κ_{lat} of GeTe is ~2.6 W/m.K, which is reduced to ~1.1 W/m.K for $Ge_{0.90}Bi_{0.10}Te$, which is ~57% reduction in κ_{lat}. We have compared the κ_{lat} of present $Ge_{0.90}Bi_{0.10}Te$ sample with previously reported high performance GeTe based materials (see **Fig.4c**). $Ge_{0.90}Bi_{0.10}Te$ sample exhibits one of lowest values of κ_{lat} among the reported GeTe based materials. The low κ_{lat} in $Ge_{1-x}Bi_xTe$ is attributed due to the increased phonon scattering of meso-scale grain boundaries, nano-scale Bi rich precipitates, defect layers and atomic-scale point defects due to mass fluctuations.

Fig. 4d illustrates the thermoelectric figure of merit, *z*T, of $Ge_{1-x}Bi_xTe$ (x = 0.00, 0.02, 0.06 & 0.10) samples as a function of temperature. Maximum zT of ~1.3 is achieved for the composition of $Ge_{0.94}Bi_{0.06}Te$ at 725 K. Error in overall zT estimation is ~10% which includes the errors from electrical conductivity, Seebeck and thermal conductivity measurement. High *z*T samples were re-measured and subjected to cyclic measurement (heating and cooling cycle), which shows a good reproducibility, that indicates prepared samples are thermally stable during thermal treatments/cycles (see **Fig. S1, SI**).

Besides high zT, materials should be mechanically stable during machining in order to use for large scale device application. We have measured mechanical properties by Vickers

Published on 18 November 2015. Downloaded on 29/11/2015 10:35:46.

Inorganic Chemistry Frontiers Accepted Manuscript

View Article Online
DOI: 10.1039/C5QI00230C

microhardness indentation method (see **Fig 5**). Generally, undoped GeTe material contains excess Ge vacancies which reduces the mechanical strength of GeTe. Bi doping reduces these Ge vacancies, and increases the rigidity of the material. Thus, Bi doping in GeTe helps to improve the mechanical property. $Ge_{0.94}Bi_{0.06}Te$ sample shows the measured microhardness value of ~165 H_V, which is considerably higher than that of the state-of-art thermoelectric materials such as, Bi_2Te_3,[19a] PbTe,[19b,19c,20a] Pb-Sn-Te,[20b] PbSe,[20c] Cu_2S,[20d] Cu_2Se[20d] and relatively comparable that of other GeTe based materials.[21]

CONCLUSION

We have synthesized the high quality ingots of $Ge_{1-x}Bi_xTe$ (x= 0-0.10) by vacuum sealed-tube melting reaction. Bi doping reduces the excess hole density in GeTe due to its aliovalent donor dopant nature. Obtained reduction in carrier density decreases the electrical conductivity and adversely increases the Seebeck coefficient in $Ge_{1-x}Bi_xTe$. Moreover, low lattice thermal conductivity of ~1.1 W/mK was achieved in $Ge_{0.90}Bi_{0.10}Te$, which is due to collective phonon scattering from meso-structured grain boundaries, nano-structured precipitates, nano-structured defect layers, and solid solution point defects. Overall, the maximum zT value of ~1.3 was obtained for the composition of $Ge_{0.94}Bi_{0.06}Te$ at 725 K, which is about ~35% higher than that of pristine GeTe. Measured Vickers micro-hardness value of $Ge_{0.94}Bi_{0.06}Te$ is 165 H_V, which is considerably higher than that of present state-of-art thermoelectric materials, such as PbTe and Bi_2Te_3.

ACKNOWLEDGEMENTS

We thank Prof. C. N. R. Rao for constant support. This work was partially supported by DRDO-JNCASR collaborative project and DAE-BRNS project (37(3)20/01/2015/BRNS). K.B. acknowledges partial support of DST Ramanujan Fellowship and Sheikh Saqr

Published on 18 November 2015. Downloaded on 29/11/2015 10:35:46.

Inorganic Chemistry Frontiers Accepted Manuscript

View Article Online
DOI: 10.1039/C5QI00230C

Laboratory. We acknowledge Devendra S. Negi for TEM sample preparation and microscopy investigation. S.R. acknowledges CSIR for PhD fellowship.

Published on 18 November 2015. Downloaded on 29/11/2015 10:35:46.

Inorganic Chemistry Frontiers Accepted Manuscript

NOTES AND REFERENCES

View Article Online
DOI: 10.1039/C5QI00230C

Published on 18 November 2015. Downloaded on 29/11/2015 10:35:46.

1. G. J. Snyder and E. S. Toberer, *Nat. Mater.*, 2008, **7**, 105.
2. L. D. Zhao, V. P. Dravid and M. G. Kanatzidis, *Energy Environ. Sci.*, 2014, **7**, 25.
3. J. Sootsman, D. Y. Chung and M. G. Kanatzidis, *Angew. Chem. Int. Ed.*, 2009, **48**, 8616.
4. (a) M. Zebarjadi, K. Esfarjani, M. S. Dresselhaus, Z. F. Ren and G. Chen, *Energy Environ. Sci.*, 2012, **5**, 5147; (b) T. Zhu, C. Fu, H. Xie, Y. Liu and X. Zhao, *Adv. Energy Mater.*, 2015, DOI: 10.1002/aenm.201500588; (c) K. Nielsch, J. Bachmann, J. Kimling and H. Böttner, *Adv. Energy Mater.*, 2011, **1**, 713; (d) C. Xiao, Z. Li, K. Li, P. Huang and Y. Xie, *Acc. Chem. Res.*, 2014, **47**, 1287.
5. (a) S. V. Faleev and F. Leonard, *Phys. Rev. B.*, 2008, **77**, 214304; (b) J. P. Heremans, V. Jovovic, E. S. Toberer, A. Saramat, K. Kurosaki, A. Charoenphakdee, S. Yamanaka and G. J. Snyder, *Science*, 2008, **321**, 554; (c) Q. Zhang, B. Liao, Y. Lan, K. Lukas, W. Liu, K. Esfarjani, C. Opeil, D. Broido, G. Chen and Z. Ren, *Proc. Natl. Acad. Sci. USA*, 2013, **110**, 13261; (d) Y. Pei, X. Shi, A. LaLonde, H. Wang, L. Chen and G. J. Snyder, *Nature*, 2011, **473**, 66; (e) W. Liu, X. Tan, K. Yin, H. Liu, X. Tang, J. Shi, Q. Zhang and C. Uher, *Phys. Rev. Lett.*, 2012, **108**, 166601; (f) L. D. Zhao, H. J. Wu, S. Q. Hao, C. I. Wu, X. Y. Zhou, K. Biswas, J. Q. He, T. P. Hogan, C. Uher, C. Wolverton, V. P. Dravid and M. G. Kanatzidis, *Energy Environ. Sci.*, 2013, **6**, 3346; (g) A. Banik, U. S. Shenoy, S. Anand, U. V. Waghmare, K. Biswas, *Chem. Mater.*, 2015, **27**, 581; (f) L. D. Hicks and M. S. Dresselhaus, *Phys. Rev. B.*, 1993, **47**, 12727.
6. K. Biswas, J. He, Q. Zhang, G. Wang, C. Uher, V. P. Dravid and M. G. Kanatzidis, *Nat. Chem.*, 2011, **3**, 160.
7. (a) K. Biswas, J. He, I. D. Blum, C. I. Wu, T. P. Hogan, D. N. Seidman, V. P. Dravid and M. G. Kanatzidis, *Nature*, 2012, **489**, 414; (b) L. D. Zhao, S. Hao, S. H. Lo, C. I. Wu, X. Zhou, Y. Lee, H. Li, K. Biswas, T. P. Hogan, C. Uher, C. Wolverton, V. P. Dravid and M. G.

Inorganic Chemistry Frontiers Accepted Manuscript

View Article Online
DOI: 10.1039/C5QI00230C

Kanatzidis, *J. Am. Chem. Soc.*, 2013, **135**, 7364; (c) B. Poudel, Q. Hao, Y. Ma, Y. Lan, A. Minnich, B. Yu, X. Yan, D. Wang, A. Muto, D. Vashaee, X. Chen, J. Liu, M. S. Dresselhaus, G. Chen and Z. Ren, *Science*, 2008, **320**, 634.

8. (a) L. D. Zhao, S. H. Lo, Y. Zhang, H. Sun, G. Tan, C. Uher, C. Wolverton, V. P. Dravid and M. G. Kanatzidis, *Nature*, 2014, **508**, 373; (b) D. T. Morelli, V. Jovovic and J. P. Heremans, *Phys. Rev. Lett.*, 2008, **101**, 035901; (c) S. N. Guin, A. Chatterjee, D. S. Negi, R. Datta and K. Biswas, *Energy Environ. Sci.*, 2013, **6**, 2603; (d) S. N. Guin, J. Pan, A. Bhowmik, D. Sanyal, U. V. Waghmare and K. Biswas, *J. Am. Chem. Soc.*, 2014, **136**, 12712.
9. E. A. Skrabek and D. S. Trimmer, *Thermoelectrics Handbook* ed. D. M. Rowe, (Boca Raton, FL: CRC), chapter 22, 1995.
10. (a)T. A. Christakudi, S. K. Plachkova and G. Ch. Christakudis, *Phys. Status Solidi A*, 1995, **147**, 211; (b) J. E. Lewis, *Phys. Status Solidi A*, 1970, **38**, 131; (c) D. H. Damon, M.S. Lubell and R. Mazelsky, *J. Phys. Chem. Solids*, 1967, **28**, 520.
11. (a) E. M. Levin, M. F. Besser and R. Hanus, *J. Appl. Phys.*, 2013, **114**, 083713; (b) H. Okamoto, Binary Alloy Phase Diagrams, II Ed., Ed. T.B. Massalski, 1990.
12. (a) T. Chattopadhyay, J. X. Boucherle and H. G. von Schnering, *J. Phys. C*, 1987, **20**, 143; (b) M. J. Polking, M.-G. Han, A. Yourdkhani, V. Petkov, C. F. Kisielowski, V. V. Volkov, Y. Zhu, G. Caruntu, A. P. Alivisatos and R. Ramesh, *Nat. Mater.*, 2012, **11**, 700; (c) P. B. Pereira, I. Sergueev, S. Gorsse, J. Dadda, E. Muller and R. P. Hermann, *Phys. Status Solidi B*, 2013, **250**,1300.
13. (a) F. D. Rosi, J. P. Dismukes and E. F. Hockings, *Electrical Eng.*, 1960, **79**, 450; (b) J. K. Lee, M. W. Oh, B. S. Kim, B. K. Min, H. W. Lee and S. D. Park, *Electron. Mater. Lett.*, 2014, **10**, 813; (c) E. M. Levin, B. A. Cook, J. L. Harringa, S. L. Bud'ko, R. Venkatasubramanian and K. Schmidt-Rohr, *Adv. Funct. Mater.*, 2011, **21**, 441; (d) S. K. Plachkova and T. I. Georgiev, *J. Phys.: Condens. Matter.*, 1993, **5**, 67; (e) J. R. Salvador, J. Yang, X. Shi, H.

Published on 18 November 2015. Downloaded on 29/11/2015 10:35:46.

Inorganic Chemistry Frontiers Accepted Manuscript

View Article Online
DOI: 10.1039/C5QI00230C

Wang and A. A. Wereszczak, *J. Solid State Chem.*, 2009, **182**, 2088; (f) L. Zhang, W. Wang, B. Ren and J. Guo, *J. Electron. Mater.*, 2013, **42**, 7.

14. (a) Y. Gelbstein, O. Ben-Yehuda, E. Pinhas, T. Edrei, Y. Sadia, Z. Dashevsky, M. P. Dariel, *J. Electron. Mater.*, 2009, **38**, 1478; (b) Y. Gelbstein, B. Dado, O. Ben-Yehuda, Y. Sadia, Z. Dashevsky, M. P. Dariel, *J. Electron. Mater.*, 2010, **39**, 2049; (c) Y. Gelbstein, J. Davidow, S. N. Girard, D. Y. Chung and M. Kanatzidis, *Adv. Energy Mater.*, 2013, **3**, 815; (d) Y. Gelbstein and J. Davidow, *Phys. Chem. Chem. Phys.*, 2014, **16**, 20120.

15. D. Wu, L.-D. Zhao, S. Hao, Q. Jiang, F. Zheng, J. W. Doak, H. Wu, H. Chi, Y. Gelbstein, C. Uher, C. Wolverton, M. G. Kanatzidis and J. He, *J. Am. Chem. Soc.*, 2014, **136**, 11412.

16. (a) S. Perumal, S. Roychowdhury, D. S. Negi, R. Datta, and Kanishka Biswas, *Chem. Mater.*, 2015, **27**, 7171; (b) F. Fahrnbauer, D. Souchay, G. Wagner and O. Oeckler, *J. Am. Chem. Soc.*, 2015, **137**, 12633; (c) T. Rosenthal, P. Urban, K. Nimmrich, L. Schenk, J. de Boor, C. Stiewe and O. Oeckler, *Chem. Mater.*, 2014, **26**, 2567; (d) J. F. Deng, J. Q. Li, R. F. Ye, X. Y. Liu, F. S. Liu and W. Q. Ao, *Journal of Alloys and Compounds*, 2014, **585**, 173.

17. K. Hoang, S. D. Mahanti and M. G. Kanatzidis, *Phys. Rev. B*, 2010, **81**, 115106.

18. (a) A. F. May, E. S. Toberer, A. Saramat and G. J. Snyder, *Phys. Rev. B* 2009, **80**, 125205; (b) L.-D. Zhao, S. -H. Lo, J. He, H. Li, K. Biswas, J. Androulakis, C. -I. Wu, T. P. Hogan, D. Y. Chung, V. P. Dravid and M. G. Kanatzidis, *J. Am. Chem. Soc.*, 2011, **133**, 20476.

19. (a) L. -D. Zhao, B. -P. Zhang, J. -F. Li, M. Zhou, W.-S. Liu and J. Liu, *J. Alloys Compd.*, 2008, **455**, 259; (b) M. S. Ablova, M. N. Vinogradova and M. I. Karklina, *Sov. Phys.–Sol. State.*, 1969, **10**, 1929; (c) A. J. Crocker and M. Wilson, *J. Mater. Sci.*, 1978, **13**, 833; (c) L.-D. Zhao, B. -P. Zhang, J. -F. Li, M. Zhou, W. -S. Liu and J. Liu, *J. Alloys Compd.*, 2008, **455**, 259.

20. (a) Y. Gelbstein, G. Gotesman, Y. Lishzinker, Z. Dashevsky and M. P. Dariel, *Scripta Materialia*, 2008, **58**, 251; (b) J. L. Cui, X. Qian and X. B. Zhao, *J. Alloy. Compd.*, 2003, **358**,

Published on 18 November 2015. Downloaded on 29/11/2015 10:35:46.

Inorganic Chemistry Frontiers Accepted Manuscript

View Article Online
DOI: 10.1039/C5QI00230C

228; (c) W. B. W. M. S. Darrow and R. Roy, *J. Mater. Sci.*, 1969, **313**; (d) L. Zhao, X. Wang, F. Y. Fei, J. Wang, Z. Cheng, S. Dou, J. Wanga and G. J. Snyder, *J. Mater. Chem. A*, 2015, **3**, 9432.

21. J. Davidow and Y. Gelbstein, *J. Eelectron. Mater.*, 2013, **42**, 1542.

Published on 18 November 2015. Downloaded on 29/11/2015 10:35:46.

Inorganic Chemistry Frontiers Accepted Manuscript

View Article Online
DOI: 10.1039/C5QI00230C

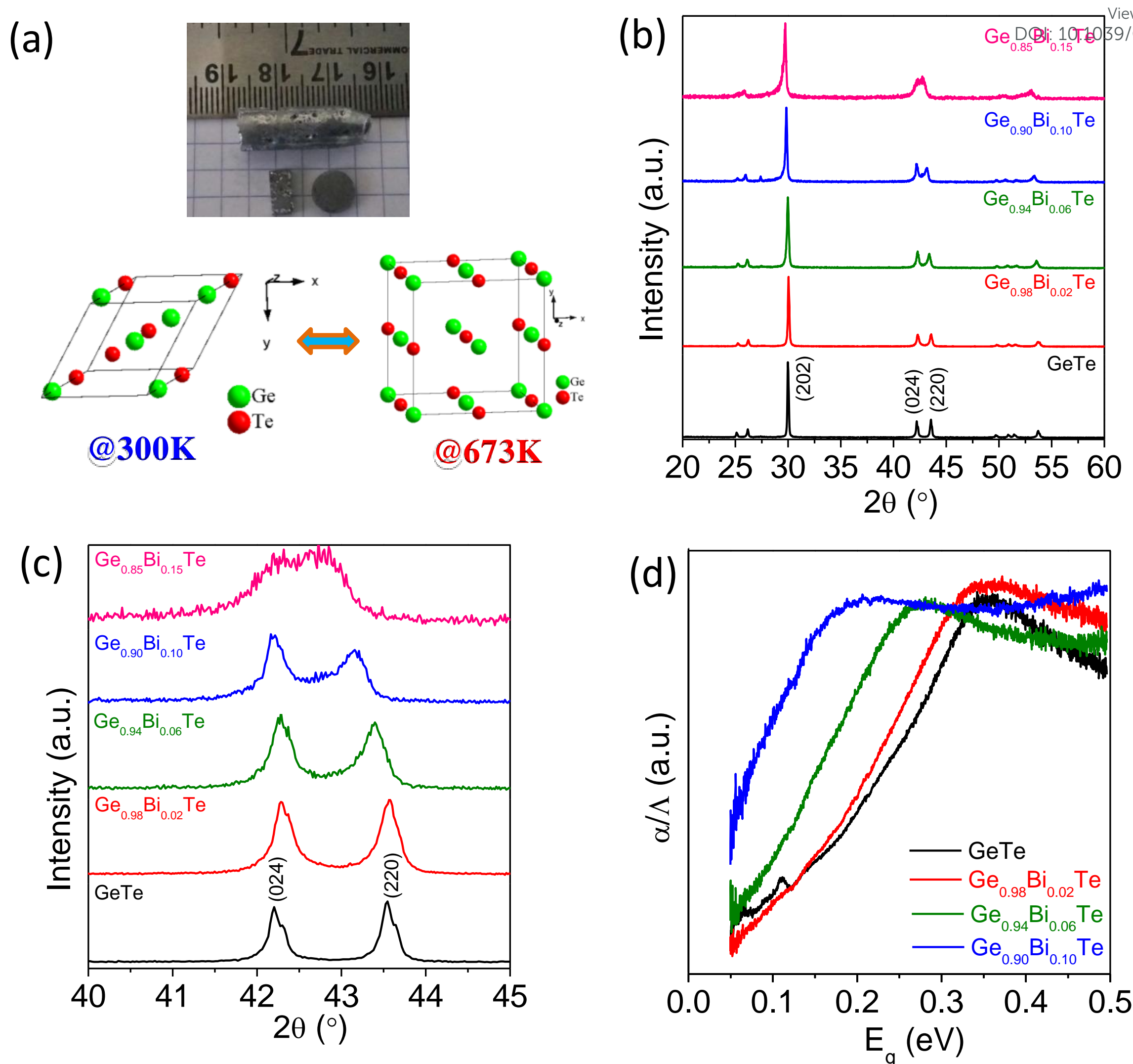

Fig. 1 (a) Photograph of high quality ingot, sliced bar and pellet, Crystal structure of GeTe, rhombohedral at 300 K and Cubic at 673 K; (b) Powder XRD patterns of $Ge_{1-x}Bi_xTe$ samples; (c) Zoomed XRD pattern of Fig.1 (b) in between the angles (2Θ) of 40˚ to 45˚, that shows the merging of (024) and (220) peaks with increasing the Bi doping; and (d) Optical absorption spectra of $Ge_{1-x}Bi_xTe$ samples.

Published on 18 November 2015. Downloaded on 29/11/2015 10:35:46.

Inorganic Chemistry Frontiers Accepted Manuscript

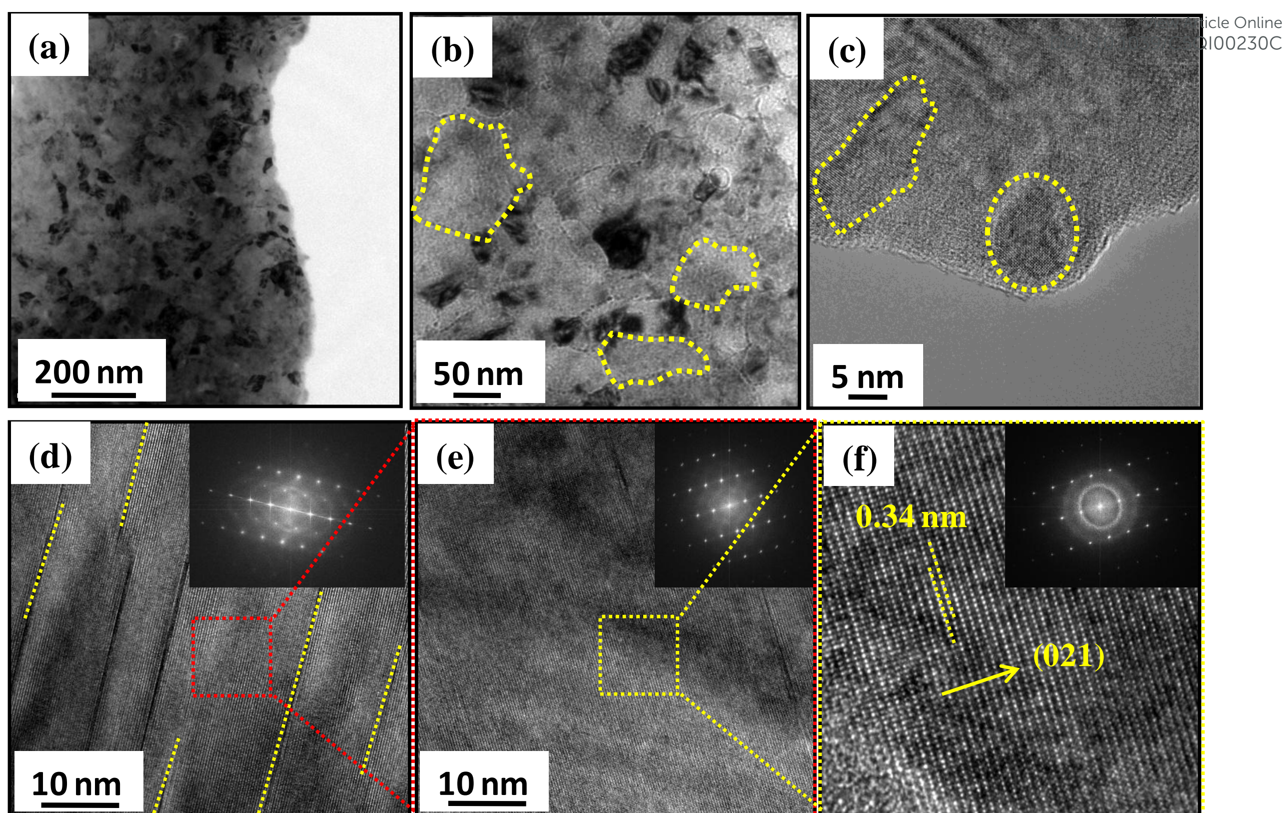

Fig. 2 (a) Low magnification TEM micrograph of $Ge_{0.90}Bi_{0.10}Te$ with Bi-rich nano-precipitates, (b) TEM image shows mesoscale grain boundaries (dotted yellow circle), (c) HRTEM images shows nanoprecipitates, (d) Parallel defect layers and their corresponding SAED pattern with diffusive spots, (e) HRTEM micrographs in the defect free region with clear SAED spots, (f) HRTEM micrograph of $Ge_{0.90}Bi_{0.10}Te$ shows a inter planar spacing of 0.34 nm (inset shows the corresponding SAED pattern).

Published on 18 November 2015. Downloaded on 29/11/2015 10:35:46.

Inorganic Chemistry Frontiers Accepted Manuscript

View Article Online
DOI: 10.1039/C5QI00230C

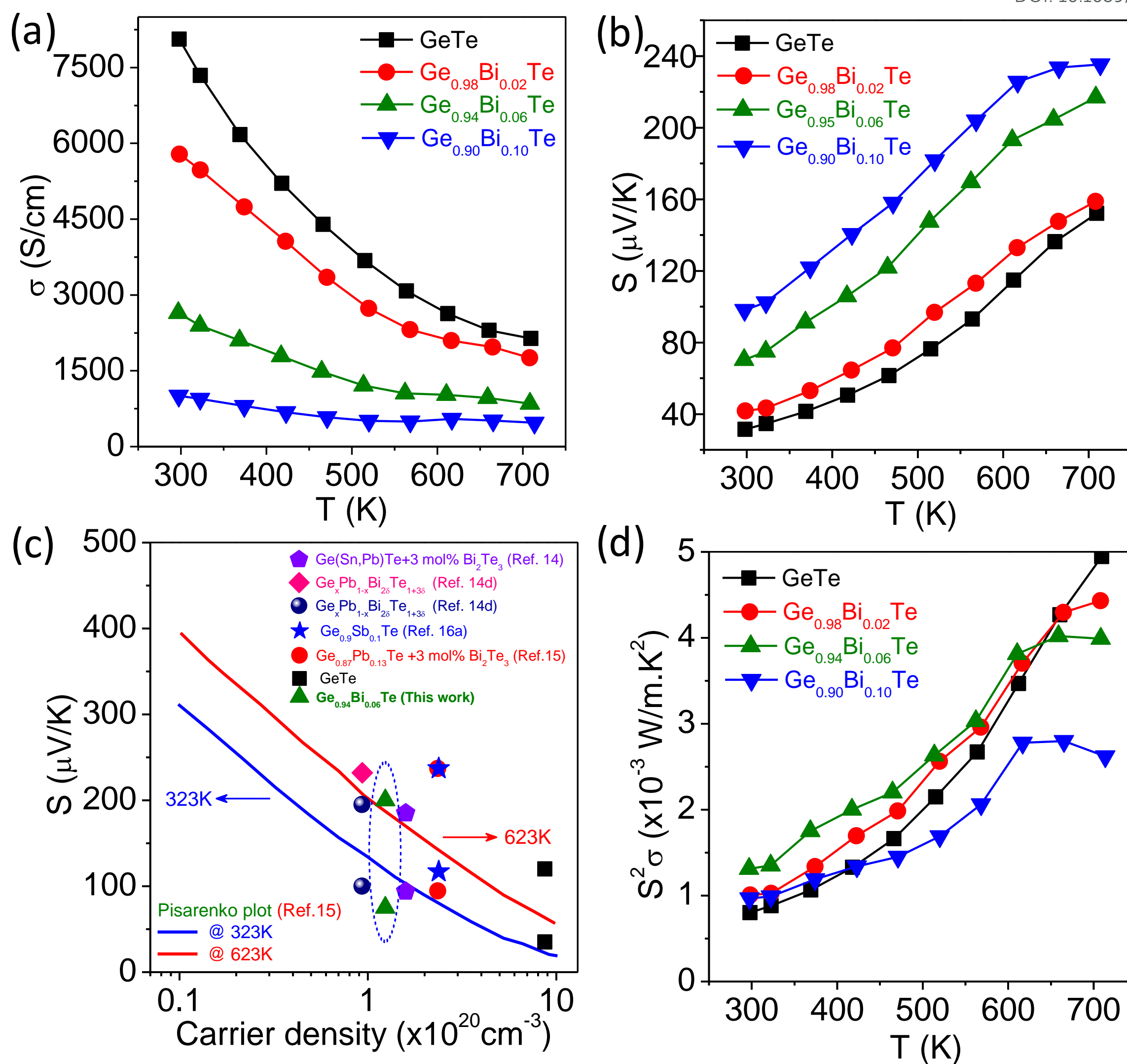

Fig. 3 Temperature dependent (a) electrical conductivity (σ) and (b) Seebeck coefficient (S) of $Ge_{1-x}Bi_xTe$ samples. (c) Pisarenko plots (S vs. n data) for $Ge_{1-x}Bi_xTe$ samples which compared with earlier reported data. (d) Temperature dependent power factor ($S^2\sigma$) of $Ge_{1-x}Bi_xTe$ samples.

Published on 18 November 2015. Downloaded on 29/11/2015 10:35:46.

Inorganic Chemistry Frontiers Accepted Manuscript

View Article Online
DOI: 10.1039/C5QI00230C

Published on 18 November 2015. Downloaded on 29/11/2015 10:35:46.

Inorganic Chemistry Frontiers Accepted Manuscript

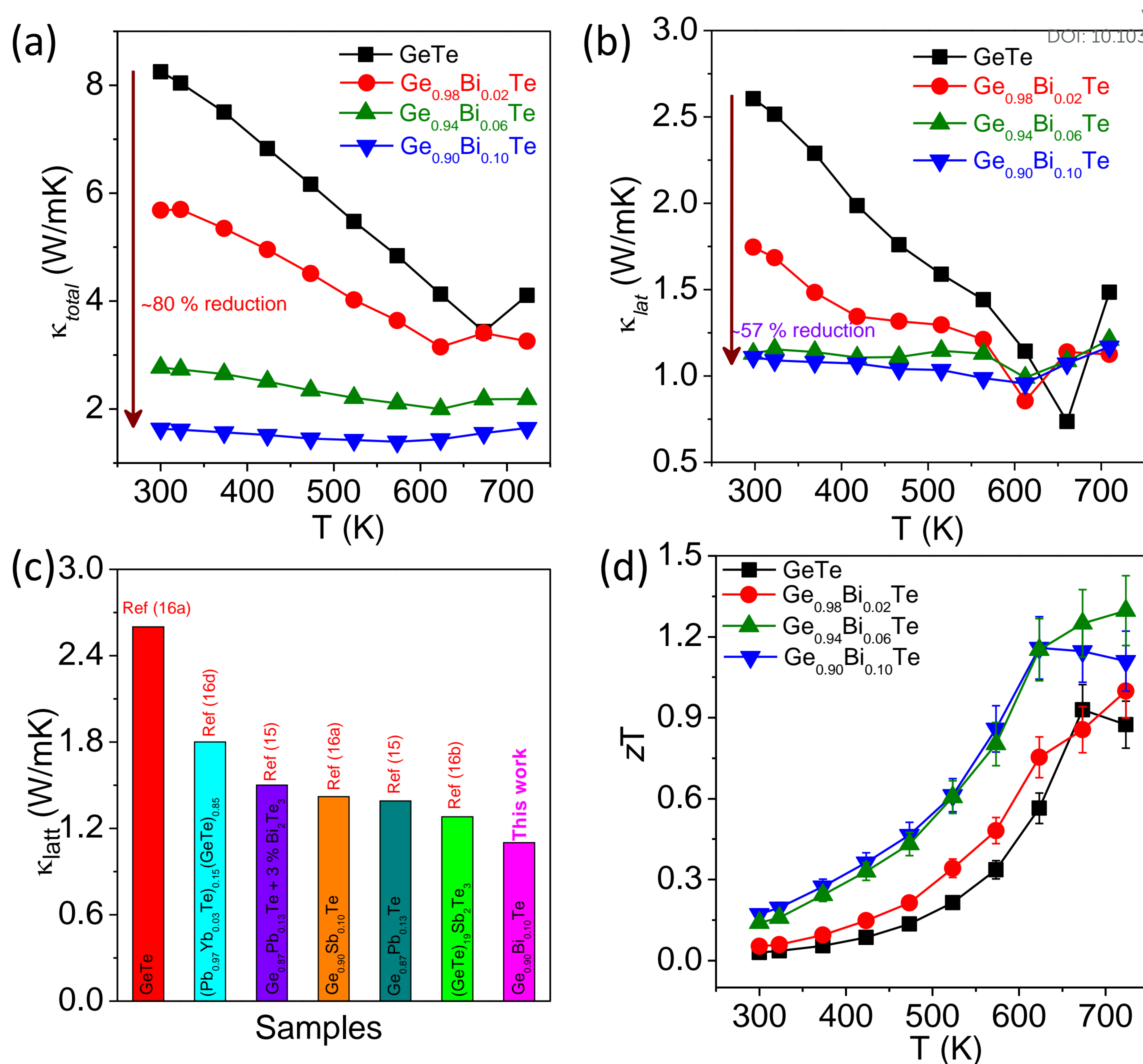

Fig. 4 Temperature dependent (a) total thermal conductivity, κ_{total}, and (b) lattice thermal conductivity, κ_{latt}, of $Ge_{1-x}Bi_xTe$ samples. (c) Comparison of the κ_{latt} of the present $Ge_{0.90}Bi_{0.10}Te$ sample with previously reported high performance GeTe based materials. (d) Dimensionless thermoelectric figure of merit, zT, of $Ge_{1-x}Bi_xTe$ samples.

View Article Online
DOI: 10.1039/C5QI00230C

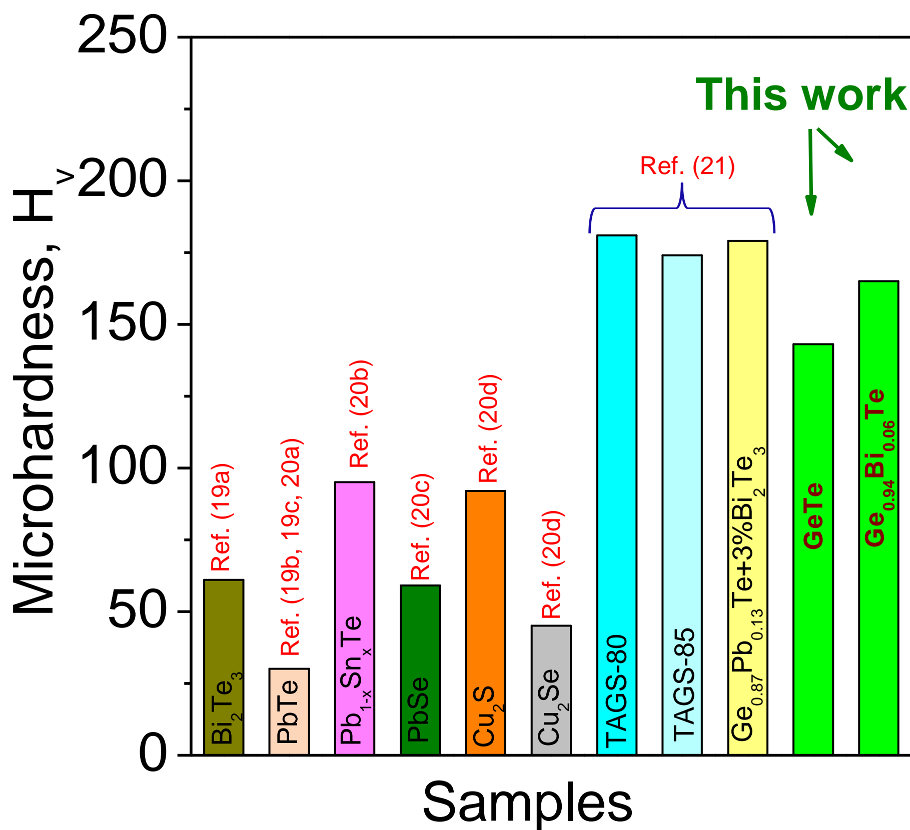

Fig. 5 Vickers microhardness values, H_V, of $Ge_{0.94}Bi_{0.06}Te$ which is compared with selected popular thermoelectric materials.

Published on 18 November 2015. Downloaded on 29/11/2015 10:35:46.

Inorganic Chemistry Frontiers Accepted Manuscript

View Article Online
DOI: 10.1039/C5QI00230C

Table of Contents

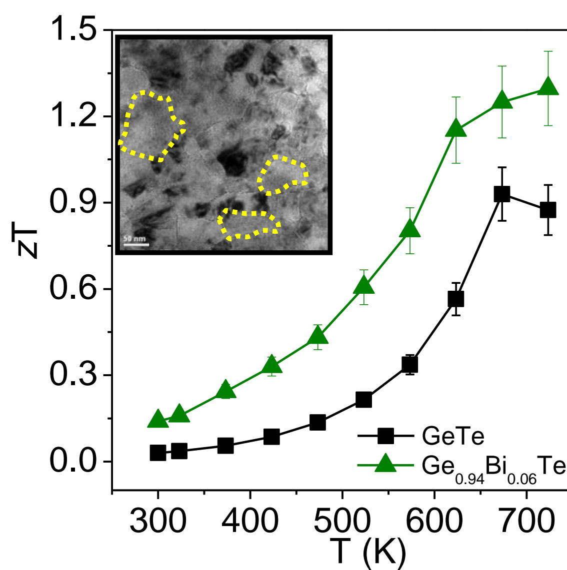

Nano/meso-structuring reduces the thermal conductivity in $Ge_{1-x}Bi_xTe$ samples, which resulted in a thermoelectric figure of merit, zT, of 1.3 in $Ge_{1-x}Bi_xTe$.

Published on 18 November 2015. Downloaded on 29/11/2015 10:35:46.

Inorganic Chemistry Frontiers Accepted Manuscript

View Article Online
DOI: 10.1039/C5QI00230C

Inorganic Chemistry Frontiers Accepted Manuscript

Published on 18 November 2015. Downloaded on 29/11/2015 10:35:46.

Biography of invited author

Kanishka Biswas obtained his MS and Ph.D degree from Solid State Structural Chemistry Unit, Indian Institute of Science (2009) and did postdoctoral research from Department of Chemistry, Northwestern University (2009-2012). He is now an Assistant Professor in New Chemistry Unit, Jawaharlal Nehru Centre for Advanced Scientific Research (JNCASR), Bangalore. He is pursuing research in solid state inorganic chemistry of metal chalcogenides, thermoelectrics, topological insulators and intergrowth 2D nanosheets. He has published 69 research papers and 3 book chapters. He is also co-author of a book entitled "Essentials of inorganic materials synthesis" published by John Wiley and Sons, Inc in 2015. He is recipient of Ramanujan Fellowship from Department of Science and Technology, India. He is an Young Affiliate of The World Academy of Sciences (TWAS) and an Associate of Indian Academy of Science, India. He is also recipient of Young Scientist Platinum Jubilee award-2015 from The National Academy of Sciences (NASI), India.